Electron beam induced modification of ZIF-8 membrane permeation properties

Journal:	*ChemComm*
Manuscript ID	CC-COM-01-2021-000252.R2
Article Type:	Communication

COMMUNICATION

Electron beam induced modification of ZIF-8 membrane permeation properties

Received 00th January 20xx,
Accepted 00th January 20xx

DOI: 10.1039/x0xx00000x

Yurun Miao,†[a] Dennis T. Lee,†[a] Matheus Dorneles de Mello,[bc] Mohammed K. Abdel-Rahman,[d] Peter Corkery,[a] J. Anibal Boscoboinik,[be] D. Howard Fairbrother,*[d] Michael Tsapatsis*[acf]

Modification of the gas permeation properties of ZIF-8 membranes using electron beam irradiation is reported. 3.8 and 3.2 fold enhancements in ideal selectivity for CO_2/N_2 and CO_2/CH_4 can be achieved with less than 1 min exposure time.

Ionizing radiation, e. g. X-ray and electron beam (e-beam), can induce various physical and chemical effects in target materials.[1-4] Radiation processing is widely applied in applications ranging from polymer modification and functionalization[5,6] to medical equipment sterilization.[7,8] However, electron induced modification of metal-organic frameworks (MOFs) has hardly been explored except for the well-documented beam damage problem in high-resolution microscopy[9] and as a means for surface activation and functionalization.[10] Recent reports show that e-beam irradiation can induce changes in the solubility of several MOFs belonging to the zeolitic imidazolate framework (ZIF) family, holding promise for their development as new resists.[11,12] In terms of the effects of ionizing radiation, X-ray induced amorphization of several ZIFs resulted primarily from photo-oxidation of Zn and subsequent breakage of Zn–N bonds[13] while gamma irradiation induced damage in MOFs depending on the type of metal in the framework.[14] However, the use of irradiation for the modification of MOFs in gas separation applications has yet to be explored. Herein we show that electron radiation can modify the gas permeation properties of a prototypical MOF, ZIF-8, as demonstrated by improved CO_2/N_2 and CO_2/CH_4 selectivity.

ZIF-8 membranes were prepared by a ligand induced permselectivation (LIPS) method as reported previously.[15] The pores of a mesoporous γ-alumina support are first blocked by dense zinc oxide using an atomic layer deposition (ALD) process.[16] The ZnO deposit is then converted to porous ZIF-8 by vapor treatment with 2-methylimidazole (2mIm). E-beam modification is accomplished by exposing the as-prepared LIPS membranes to the output of an electron flood gun operating at 2 kV (Fig. 1 and S1). The irradiation time was varied between 10 s and 100 min to study the effect of electron dose on gas permeation behavior. Irradiation times of 10 s, 1 min, 5 min and 100 min correspond to electron dose of 0.017, 0.1, 0.5 and 10 mC/cm^2, respectively. At an incident energy of 2 kV, electrons can penetrate up to 200 nm in ZIF-8 and 60 nm in γ-alumina, as suggested by a Monte Carlo simulation using Casino software (Fig. S2).[17] Since the thickness of the γ-alumina layer containing ZIF-8 is ca. 5 µm, the electron irradiation is therefore expected to be surface sensitive and affect only the topmost layers.

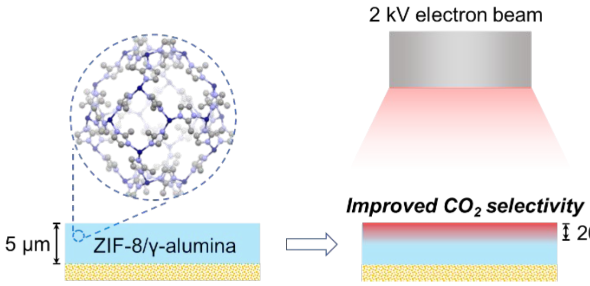

Fig. 1. Schematic of electron beam treatment of ZIF-8 membranes, showing the irradiation induced modification of the topmost layer.

The single gas permeation behavior of the membranes tested before and after e-beam exposure are shown in Fig. 2. CO_2, N_2 and CH_4 permeances of LIPS membranes before irradiation are 1.9, 1.1 and 1.4×10^{-7} mol m^{-2} Pa^{-1} s^{-1}, respectively, corresponding to an ideal selectivity of 1.64 for CO_2/N_2 and 1.33 for CO_2/CH_4. After e-beam irradiation, a general trend of

a. Department of Chemical and Biomolecular Engineering & Institute for NanoBioTechnology, Johns Hopkins University, 3400 N. Charles Street, Baltimore, MD 21218 (USA). Email: tsapatsis@jhu.edu
b. Center for Functional Nanomaterials, Brookhaven National Laboratory, Upton, NY 11973 (USA).
c. Catalysis Center for Energy Innovation, University of Delaware, Newark, DE 19716 (USA).
d. Department of Chemistry, Johns Hopkins University, 3400 N. Charles Street, Baltimore, MD 21218 (USA). Email: howardf@jhu.edu
e. Materials Science and Chemical Engineering Department, Stony Brook University, Stony Brook, NY 11790 (USA).
f. Applied Physics Laboratory, Johns Hopkins University 11100 Johns Hopkins Road, Laurel, MD 20723 (USA).
† These authors contributed equally to this work.
Electronic Supplementary Information (ESI) available. See DOI: 10.1039/x0xx00000x

reduced permeation is observed in all gases, among which CO_2 is least affected at short irradiation times. For example, the permeance of CO_2 for a membrane exposed for 1 min slightly decreases to 1.5×10^{-7} mol m^{-2} Pa^{-1} s^{-1}, while those of N_2 and CH_4 drop to 2.4 and 3.6×10^{-8} mol m^{-2} Pa^{-1} s^{-1} respectively. The CO_2/N_2 and CO_2/CH_4 selectivity of 6.3 and 4.2 after e-beam irradiation marks a 3.8- and 3.2-fold increase, respectively. At longer irradiation times of 5 and 100 min, permeances of all gases decrease dramatically to ca. 1% of the original values, suggesting significant structural changes and pore blocking possibly due to e-beam induced crosslinking of the imidazolate ligands.

The permeation behavior of a membrane after e-beam exposure for 1 min was also tested at elevated temperatures (Fig. 2 (c) and (d)). The CO_2 and N_2 permeances measured at 80 °C are 1.8×10^{-7} and 4.2×10^{-8} mol m^{-2} Pa^{-1} s^{-1}, respectively, corresponding to a CO_2/N_2 selectivity of 4.2. The CO_2/N_2 selectivity then returns to 7.0 upon cooling to room temperature (i.e., 23 °C), mainly due to the decrease in N_2 permeance. The temperature-dependent variation in N_2 permeance is observed again during a repeated heating/cooling process, and the recorded permeances and selectivities are reproduced at each temperature, confirming the stability of the e-beam treated membrane during 23-80 °C temperature cycling over the period of testing (ca. 2 weeks).

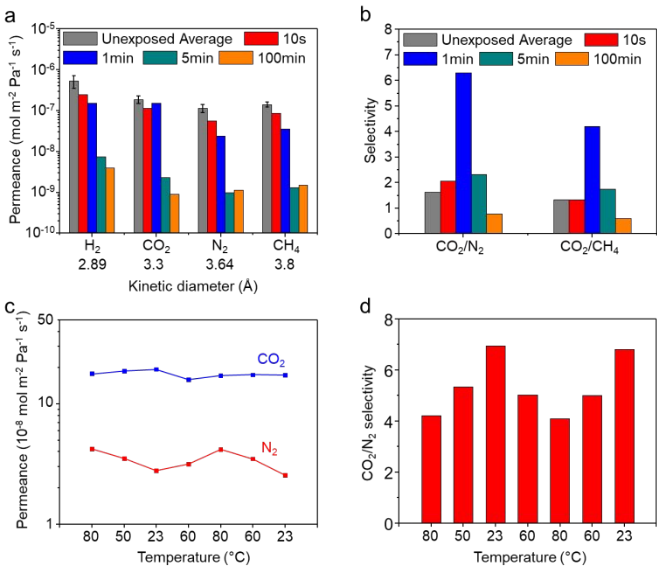

Fig. 2. (a) Single gas permeances and (b) CO_2/N_2 and CO_2/CH_4 ideal selectivities of LIPS ZIF-8 membranes before and after electron beam exposure. (c) CO_2 and N_2 permeances at various temperatures in the 23-80 °C range of a membrane exposed to e-beam for 1 min, and (d) the corresponding ideal selectivities for CO_2/N_2. Permeances for each gas are measured over a period of 24 h at each temperature, respectively. The data points in (c) are from stabilized permeances with less than 10% variation in each on-stream stability test.

The surface morphology of e-beam irradiated membranes was examined by scanning electron microscopy (SEM). As shown in Fig. 3(a-c) and S3, variations exist from sample to sample and no significant change can be attributed to e-beam. X-ray diffraction (XRD) patterns also clearly show ZIF-8 peaks in all samples including the membrane exposed for 100 min, and provide no evidence for the formation of new crystalline species (Fig. 3(d)). Due to the small thickness and γ-alumina-confinement-induced disorder of LIPS ZIF-8 membranes, the relative intensities of ZIF-8 reflections are low and vary significantly from sample to sample. Therefore, they cannot be used as a quantitative measure of structural changes induced by the e-beam. To further investigate the structural transformation induced by e-beam treatment, grazing incidence small angle X-ray scattering (GISAXS) experiment was performed on fresh and irradiated 100-nm thick ZIF-8 films prepared by 2mIm vapor treatment of ZnO deposited on silicon wafers.[18] The peak intensity for the ZIF-8 film exposed to e-beam for 100 min is significantly reduced compared to those for fresh ZIF-8 and ZIF-8 treated for 1 min (Fig. S4), indicating dose-dependent amorphization induced by e-beam treatment. The difference in crystallinity of the well-crystalized silicon-supported thin film samples after e-beam irradiation supports the idea that the changes responsible for the selectivity enhancement in LIPS ZIF-8 membranes do not affect the entire ZIF-8 deposit but are localized to the topmost surface layers.

It has been reported that a small decrease in unit cell volume is observed in ZIFs irradiated by X-ray before they are completely amorphized, suggesting structure densification accompanied by increasing micro-strain.[13] Structural transitions, such as lattice stiffening induced by an electric field, can significantly alter the permeation behavior of ZIF-8 membranes.[19-21] Therefore, it is possible that low-dose e-beam irradiation causes small structural modifications in ZIF-8 that lead to the improved CO_2/N_2 selectivity, whereas in the case of high-dose irradiation the pores are mostly blocked due to densification.

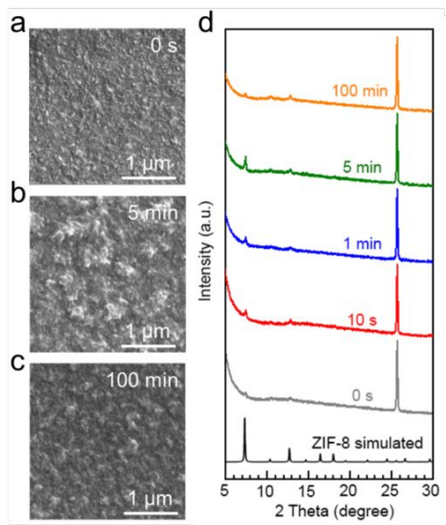

Fig. 3. (a, b and c) Top-view SEM images and (d) XRD patterns of LIPS ZIF-8 membranes before and after electron beam exposure. The insets in panels (a, b and c) are digital photographs of the corresponding membranes.

To investigate the changes caused by e-beam irradiation on the surface of ZIF-8, we collected X-ray photoelectron spectra (XPS) from ZIF-8 thin films irradiated by an *in situ* generated e-beam (Fig. 4). XPS of the non-irradiated film is consistent with literature reports.[22-24] The N 1s spectrum shows a single peak at

398.8 eV that can be assigned to C-N/C=N bond in the imidazole ring.[22] After irradiation, while no significant changes are observed in the binding energy of Zn 2p (Fig. S5), a small shoulder appears at 401.2 eV in the N 1s spectrum (Fig. 4(b)). This change indicates the formation of N-H bonds[25] due to the electron induced cleavage of either the Zn-N bond[12] or the C-N/C=N bond[26] in the imidazole ring. One possibility is that the breakage of bonds frees the transient nitrogen species to recombine with protons in a cascade of radical reactions induced by the e-beam, and the presence of N-H bonds in open pores increases the adsorption of CO_2 in ZIF-8, leading to the improved CO_2 selectivity in permeation measurements,[27,28] although the crosslinking of imidazolate ligands becomes dominant and causes pore blocking at increased doses. It should be noted that the area ratios of N-H bond relative to C-N/C=N with respect to Zn 2p is still very small (0.05 vs. 0.67 in Fig. 4(c), i.e., 8% vs. 92%) after an electron dose of 32.4 mC/cm^2, much higher than the highest electron dose used in the permeation experiments. Therefore, it is likely that any modification to the chemical bonding in the ZIF-8 responsible for the significant change in permeation behavior is much less severe.

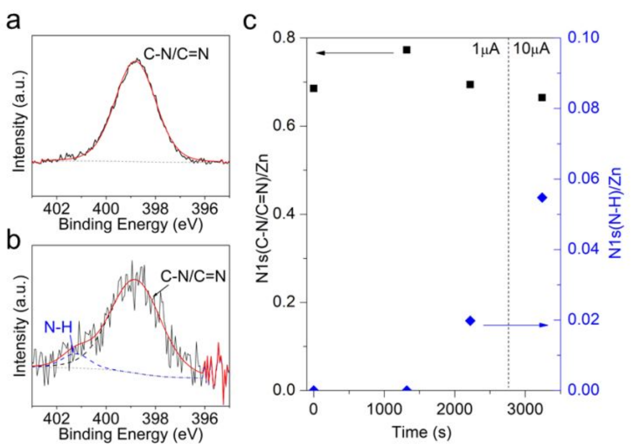

Fig. 4. N 1s XPS spectra from ZIF-8 thin film before (a) and after (b) 54 min *in situ* e-beam irradiation, and (c) evolution of signals with time of e-beam exposure corresponding to the two nitrogen species with respect to the intensity of Zn 2p. Dashed line in (c) marks where the current is increased from 1 μA to 10 μA.

In conclusion, it is demonstrated that electron beam irradiation can be used to alter the permeation properties of MOF membranes. Low dose exposure for less than 1 min increases CO_2 selectivity, while high dose exposure leads to reduced permeance and selectivity.

This material is based upon work supported by the U.S. Department of Energy, Office of Science, Office of Basic Energy Sciences, Division of Chemical Sciences, Geosciences and Biosciences under Award DE-SC0021212 and Award DE-SC0021304. XPS data collection and analysis was partially supported from the Catalysis Center for Energy Innovation, an Energy Frontier Research Center funded by the U.S. Department of Energy, Office of Science, Office of Basic Energy Sciences under Award No. DE-SC0001004. The authors thank Dr. Rachel Thorman for her assistance with the e-beam irradiation experiments.

Notes and references

1 R. F. Egerton, P. Li and M. Malac, *Micron*, 2004, **35**, 399–409.
2 I. G. Gonzalez-Martinez, A. Bachmatiuk, V. Bezugly, J. Kunstmann, T. Gemming, Z. Liu, G. Cuniberti and M. H. Rümmeli, *Nanoscale*, 2016, **8**, 11340–11362.
3 J. Wang, C. Morin, L. Li, A. P. Hitchcock, A. Scholl and A. Doran, *J. Electron Spectros. Relat. Phenomena*, 2009, **170**, 25–36.
4 J. I. Goldstein, D. E. Newbury, J. R. Michael, N. W. M. Ritchie, J. H. J. Scott and D. C. Joy, *Microscopy and X-Ray Microanalysis*, 2018.
5 A. G. Chmielewski, M. Haji-Saeid and S. Ahmed, *Nucl. Instruments Methods Phys. Res. Sect. B Beam Interact. with Mater. Atoms*, 2005, **236**, 44–54.
6 S. Hasegawa, S. Takahashi, H. Iwase, S. Koizumi, N. Morishita, K. Sato, T. Narita, M. Ohnuma and Y. Maekawa, *Polymer (Guildf).*, 2011, **52**, 98–106.
7 D. de Cassan, A. L. Hoheisel, B. Glasmacher and H. Menzel, *J. Mater. Sci. Mater. Med.*, 2019, **30**, 1–11.
8 B. L. Proffen, G. S. Perrone, B. C. Fleming, J. T. Sieker, J. Kramer, M. L. Hawes, G. J. Badger and M. M. Murray, *J. Orthop. Res.*, 2015, **33**, 1015–1023.
9 C. Wiktor, M. Meledina, S. Turner, O. I. Lebedev and R. A. Fischer, *J. Mater. Chem. A*, 2017, **5**, 14969–14989.
10 K. Ahlenhoff, C. Preischl, P. Swiderek and H. Marbach, *J. Phys. Chem. C*, 2018, **122**, 26658–26670.
11 S. Conrad, P. Kumar, F. Xue, L. Ren, S. Henning, C. Xiao, K. A. Mkhoyan and M. Tsapatsis, *Angew. Chemie Int. Ed.*, 2018, **57**, 13592–13597.
12 M. Tu, B. Xia, D. E. Kravchenko, M. L. Tietze, A. J. Cruz, I. Stassen, T. Hauffman, J. Teyssandier, S. De Feyter, Z. Wang, R. A. Fischer, B. Marmiroli, H. Amenitsch, A. Torvisco, M. de J. Velásquez-Hernández, P. Falcaro and R. Ameloot, *Nat. Mater.*, 2021, **20**, 93–99.
13 R. N. Widmer, G. I. Lampronti, N. Casati, S. Farsang, T. D. Bennett and S. A. T. Redfern, *Phys. Chem. Chem. Phys.*, 2019, 12389–12395.
14 C. Volkringer, C. Falaise, P. Devaux, R. Giovine, V. Stevenson, F. Pourpoint, O. Lafon, M. Osmond, C. Jeanjacques, B. Marcillaud, J. C. Sabroux and T. Loiseau, *Chem. Commun.*, 2016, **52**, 12502–12505.
15 X. Ma, P. Kumar, N. Mittal, A. Khlyustova, P. Daoutidis, K. Andre Mkhoyan and M. Tsapatsis, *Science*, 2018, **361**, 1008–1011.
16 I. Stassen, M. Styles, G. Grenci, H. Van Gorp, W. Vanderlinden, S. De Feyter, P. Falcaro, D. De Vos, P. Vereecken and R. Ameloot, *Nat. Mater.*, 2016, **15**, 304–310.
17 D. Drouin, A. R. Couture, D. Joly, X. Tastet, V. Aimez and R. Gauvin, *Scanning*, 2007, **29**, 92–101.
18 M. Hayashi, D. T. Lee, M. Dorneles de Mello, A. Boscoboinik and M. Tsapatsis, *Angew. Chemie Int. Ed.*, 2021, **11973**, 1–6.
19 H. Bux, F. Liang, Y. Li, J. Cravillon, M. Wiebcke and J. Caro, *J. Am. Chem. Soc.*, 2009, **131**, 16000–16001.
20 H. Bux, C. Chmelik, J. M. Van Baten, R. Krishna and J. Caro, *Adv. Mater.*, 2010, **22**, 4741–4743.
21 A. Knebel, B. Geppert, K. Volgmann, D. I. Kolokolov, A. G. Stepanov, J. Twiefel, P. Heitjans, D. Volkmer and J. Caro, *Science (80-.).*, 2017, **358**, 347–351.
22 J. Li, M. Chen, D. A. Cullen, S. Hwang, M. Wang, B. Li, K. Liu, S. Karakalos, M. Lucero, H. Zhang, C. Lei, H. Xu, G. E. Sterbinsky, Z. Feng, D. Su, K. L. More, G. Wang, Z. Wang and G. Wu, *Nat. Catal.*, 2018, **1**, 935–945.
23 W. Wu, J. Su, M. Jia, Z. Li, G. Liu and W. Li, *Sci. Adv.*, 2020, **6**, 1–8.
24 S. Bhattacharyya, S. H. Pang, M. R. Dutzer, R. P. Lively, K. S. Walton, D. S. Sholl and S. Nair, *J. Phys. Chem. C*, 2016, **120**, 27221–27229.

25 G. Xue, Q. Dai and S. Jiang, *J. Am. Chem. Soc.*, 1988, **110**, 2393–2395.
26 R. Meißner, L. Feketeová, A. Ribar, K. Fink, P. Limão-Vieira and S. Denifl, *J. Am. Soc. Mass Spectrom.*, 2019, **30**, 2678–2691.
27 L. Xiang, L. Sheng, C. Wang, L. Zhang, Y. Pan and Y. Li, *Adv. Mater.*, 2017, **29**, 1606999.
28 K. Eum, M. Hayashi, M. D. De Mello, F. Xue, H. T. Kwon and M. Tsapatsis, *Angew. Chemie Int. Ed.*, 2019, **58**, 16390–16394.